# Dynamical Screening at a Metal Surface Probed by Second-Harmonic Generation

K. J. Song, D. Heskett, H. L. Dai, A. Liebsch,[a] and E. W. Plummer
*Laboratory for Research in the Structure of Matter, University of Pennsylvania, Philadelphia, Pennsylvania 19104*
(Received 10 March 1988)

The surface sensitivity of second-harmonic generation has been utilized to measure the spatial and frequency dependence of the local field generated at the surface of a nearly free-electron metal by an external electromagnetic field. The second-harmonic signal as a function of film thickness for a thin layer of alkali metal deposited onto a single-crystal substrate produces a direct image of the damped oscillatory longitudinal field generated in the metal in response to the external field.

PACS numbers: 68.35.Ja, 42.65.Ky, 78.65.Ez

The dynamical response of electrons at a metal surface to a time-varying external probe is intimately related to many physical and chemical properties of the surface such as the sticking coefficient of incoming atoms or molecules, the nature of the van der Waals forces at the surface, energy transfer from excited states of adsorbed molecules, optical reflectance and absorption, nonlinear surface optical response, surface plasmon dispersion, and the surface photoelectric effect. Because of this broad range of applications, extensive theoretical investigations of the dynamical screening properties of a semi-infinite interacting electron gas have been carried out.[1] The quantity of central interest in the above phenomena is the spatial distribution of the frequency-dependent screening density in the surface region. Below the plasma frequency ($\omega_p$), the screening charge at simple-metal surfaces is typically concentrated within a few angstroms of the surface with weaker Friedel-type oscillations extending into the metal. The most direct evidence so far of this dynamical response of electrons at a metal surface is the local field enhancement that has been observed in the surface photoelectric effect for several nearly free-electron metals.[1-3]

We will show in this paper that the nonlinear optical response from a surface or interface can be used to probe the microscopic characteristics of the dynamic screening field at a surface. In particular, we demonstrate that this technique can provide a direct image of the dynamic *Friedel oscillations* which are a consequence of the coupling of transverse and longitudinal fields at a metal surface.

Nonlinear optical processes are becoming more widely used as probes of surfaces. Second-harmonic generation (SHG) has surely established itself as a tool capable of yielding valuable information about the surface chemistry[4-6] as well as the geometry at the surface.[7,8] In general, the complexity of the nonlinear optical process compared to a linear process is compensated by the increased surface sensitivity. In a medium with inversion symmetry, SHG is forbidden in the bulk within the electric dipole approximation. The surface, on the other hand, is noncentrosymmetric allowing for a dipole-allowed SH signal, creating an inherent surface sensitivity for SHG.

Figure 1 shows the SHG from a Rb film grown on a Ag(110) surface as a function of the film thickness, for two different incident wavelengths 532 and 1064 nm. At 1064 nm, there is an increase of about 1600 in the SH signal with respect to the clean Ag surface for 1-monolayer coverage of Rb. At 532 nm, a monolayer of Rb enhances the substrate SH signal by only a factor of about 10. After this increase, the SH signal shows a gradual decrease in intensity as the film thickness increases (dashed line in the 1064-nm curve), modulated by short-wavelength oscillations. The wavelengths of these damped oscillations are 22 Å for 1064-nm and 12 Å for 532-nm radiation, respectively. Subsequent arguments will show that these oscillations in the SH signal as a function of film thickness are a result of the longitudinal density waves set up by the external driving field.

The experiments were carried out in a standard UHV chamber with a base pressure in the low $10^{-10}$-Torr range, with use of a $Q$-switched Nd-doped yttrium-aluminum-garnet laser whose output at 1064 nm was frequency doubled by a potassium dihydrogen phosphate (KDP) crystal to produce a beam of 532-nm light when needed. The details of this setup have been reported previously.[8,9] The film thickness was determined by measurement of the rate of Rb evaporation from the source with a line of sight mass spectrometer, simultaneously with the SH signal, and then calibration of this flux to the film thickness by use of the work-function change, thermal desorption spectra, and photoyield intensity.[9]

The SH signal shown in Fig. 1 is very sensitive to the perfection of the film and to the smoothness of the substrate. Experiments conducted on a freshly ion-bombarded but not annealed Ag substrate showed the same dramatic increase in SH signal as Rb was adsorbed, but the short-wavelength oscillations were missing, presumably because of the nonuniformity in film thickness. The measurements shown in Fig. 1 were made with the incident light 60° from the normal and $p$ polarized so that there was an appreciably strong component of the light vector normal to the surface. The magnitude but not the wavelength of the oscillations depends upon the angle of

 

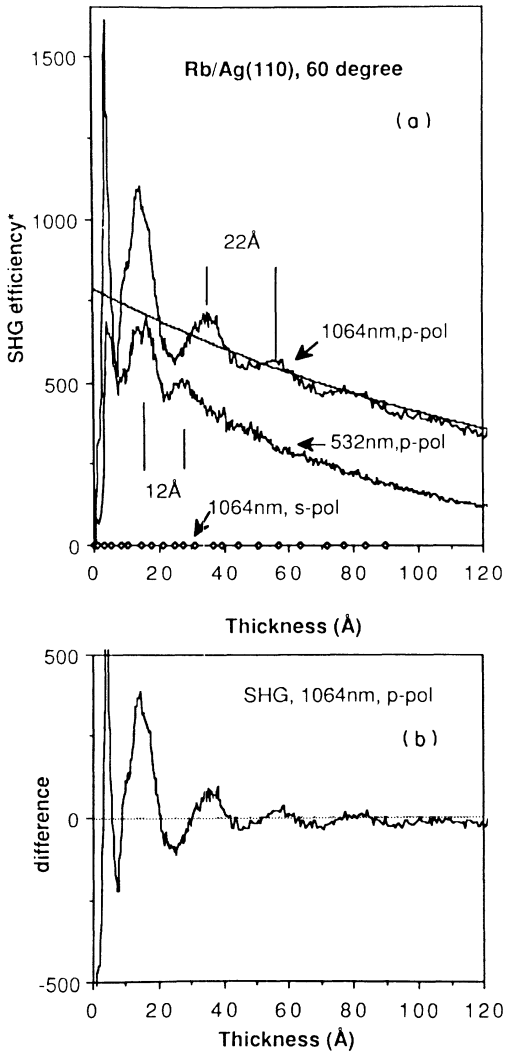


FIG. 1. (a) SH signal as a function of Rb film thickness for two different wavelengths for $p$-polarized light. The SH signal is normalized to the Ag(110) signal at 1064 nm, while the efficiency is the SH energy flux divided by the incident energy flux squared. The O's are the 1064-nm data for $s$-polarized light. The angle of incidence is 60°. (b) The oscillatory part of the 1064-nm SH signal after the smoothly varying background shown by the dashed line in (a) has been subtracted.

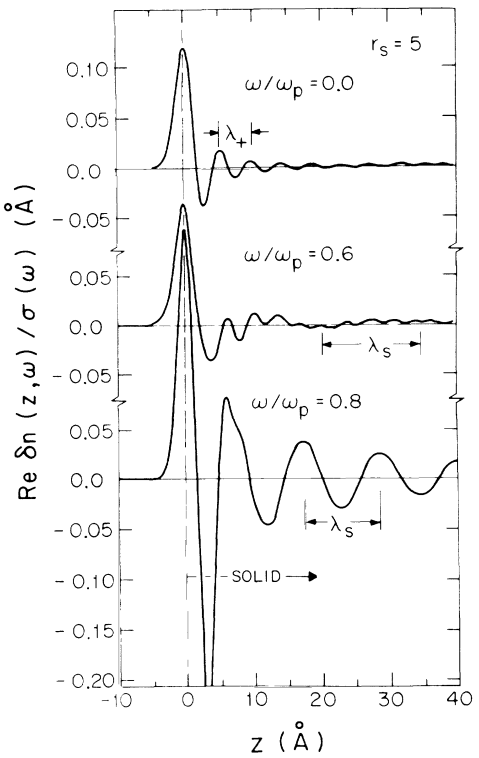


FIG. 2. Real part of the normalized density (Ref. 11) induced at a metal surface by a uniform electric field oriented normal to the surface ($r_s = 5a_0$). The positive background occupies the half-space $z > 0$. The principal short- and long-wavelength oscillations are marked by $\lambda_+$ and $\lambda_s$, respectively.

incidence (measurements were made between 30° and 60°). As a check on the presence of surface roughness in the Rb films, measurements were made with $s$-polarized light. With $s$ polarization there is almost no measurable signal from the clean Ag or from the adsorbed Rb film [see Fig. 1(a)]. This proves that the films are flat and that the oscillations seen with $p$-polarized light are not a consequence of surface morphology. If the films are grown at an elevated temperature, ~170 K, small islands or balls are formed and the oscillations and polarization dependence seen in Fig. 1 are destroyed.

There is a fundamental difference between the screening at a surface and in the bulk for simple metals, since at a surface a long-wavelength transverse external electromagnetic field can induce a short-wavelength longitudinal response.[1] In Fig. 2, the calculated linearly induced surface density is shown for various frequencies of the incident radiation. The bulk density $n$ corresponds to $r_s = 5a_0$ $\{n = (4\pi r_s^3/3)^{-1}\}$, quite close to that of Rb ($r_s = 5.2a_0$). The positive ionic charges were treated within the jellium model, and the time-dependent density-functional approach[10] was used to describe electron-electron interactions in the presence of the external field.[11] In the static limit, the screening cloud consists of a main peak in the region where the equilibrium density profile smoothly decreases from the bulk value. Because of the finite momentum cutoff at $k_F$, weak Freidel oscillations with a wavelength $\lambda = \pi/k_F = \lambda_F/2$ extend into the interior of the metal.

At finite frequencies, the main peak of the screening density takes on a more complicated, dipolar shape and the tail in the interior consists of a superposition of several Friedel-type oscillations.[12] Close to $0.8\omega_p$, the electron-hole pair excitations, which contribute to the surface screening process, show a resonance which may be viewed as a damped collective mode. This resonance

leads to a sharp peak in the imaginary part of the first moment $d(\omega)$ of the linearly induced screening density and, consequently, to a strong enhancement of the surface photoabsorption cross section.[1-3]

The oscillations of the induced density in the interior, which are of primary interest in the present work, arise for two reasons. First, according to the well-known bulk excitation spectrum shown in Fig. 3, the electron-hole pair continuum is limited by the lines $q_{\pm}(\omega) = \pm k_F + (k_F^2 + 2m\omega/\hbar)^{1/2}$ which correspond to intraband excitations from the Fermi energy to free-electron states at $E_F + \hbar\omega$ (excitations from occupied states at $E_F - \hbar\omega$ to the Fermi energy lie within this continuum). These sharp boundaries of the range of allowed bulk transitions lead to oscillations of wavelength $\lambda_{\pm} = 2\pi/q_{\pm}(\omega)$. In the static limit, $\lambda_+$ approaches $\lambda_F/2$, whereas $\lambda_-$ becomes infinite. The second type of oscillations is related to the presence of the surface. Since the densities shown in Fig. 2 are induced by a time-dependent uniform electric field normal to the surface, one can show that oscillations at $q = 2k_F$ are present at all frequencies. The screening of these oscillations then leads to a branch $q_s(\omega)/k_F = \hbar\omega/2E_F$.[12,13]

The initial dramatic rise of the SH signal upon adsorption of about 1 monolayer of Rb has been observed also for other alkali overlayers on Rh (Ref. 6) and Ag.[9] It is presumably caused by intra-atomic resonances, either within the broadened alkali valence orbitals or between this orbital and the next unoccupied level. Here, we will not discuss this very interesting effect further, but focus instead on the oscillatory decline of this signal as the thickness of the Rb layer is increased. We propose the following model in order to explain this part of the spectra. As pointed out above, the interaction of the incident electromagnetic wave with the metal electrons causes density fluctuations of the type shown in Fig. 2. As a result, a longitudinal electric field nearly normal to the surface is setup in the Rb film. This field varies in time at the frequency $\omega$ and spatially it exhibits the same oscillations as the linearly induced density. Calculations of the SHG from the surface of an electron gas[14] show that the signal is generated within a few Thomas-Fermi screening lengths of the surface, especially for small values of $\omega/\omega_p$. This means that the SHG can be modeled via a local second-order susceptibility $\chi^{(2)}$ at each interface, $\chi_1^{(2)}$ at the vacuum-alkali interface (1) and $\chi_2^{(2)}$ at the alkali-Ag interface (2). With this assumption, the SH signal $I(2\omega)$ can be written as

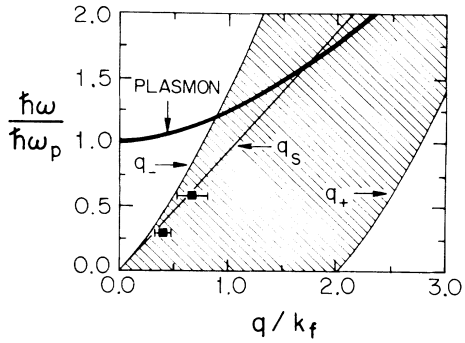


FIG. 3. The excitation spectrum for a free-electron metal with the density of Rb. The shaded region is the electron-hole pair continuum and the heavy line is the bulk plasmon dispersion. Three critical $q(\omega)$ branches are shown by the lines $q_s$, $q_+$, and $q_-$ (see text). The experimental points denote the wave vectors corresponding to the oscillations shown in Fig. 1 for 532- and 1064-nm radiation.

$$I(2\omega) \propto |E_T^2(\omega)\chi_1^{(2)} + E_T'^2(\omega)\chi_2^{(2)} + E_L'(\omega)E_T'(\omega)\chi_2^{(2)} + E_L'^2(\omega)\chi_2^{(2)}|^2, \quad (1)$$

where $E_T(\omega)$ and $E_T'(\omega)$ are the effective transverse fields at the two interfaces and $E_L'(\omega)$ denotes the longitudinal field generated at interface 1 by the incident transverse wave, evaluated at interface 2. *We have ignored the effects of the longitudinal wave created at interface 2 on the signal at interface 1, but it would not make a fundamental difference in the interpretation that follows.* If we neglect terms of order $\{E_L'(\omega)\}^2$, Eq. (1) reduces to

$$I(2\omega) \propto |E_T^2(\omega)\chi_1^{(2)} + E_T'^2(\omega)\chi_2^{(2)}|^2 + 2\mathrm{Re}\{[E_T^2(\omega)\chi_1^{(2)} + E_T'^2(\omega)\chi_2^{(2)}]^* E_L'(\omega)E_T'(\omega)\chi_2^{(2)}\}. \quad (2)$$

Since the wavelengths of the transverse waves are long compared to the variations in film thickness, none of the terms in Eq. (2) change rapidly with film thickness except the longitudinal field $E_L'(\omega)$. The reduction of the transmitted transverse field $E_T'(\omega)$ as a function of film thickness due to the absorption of the incident light produces the gradual decline in the SH signal seen in Fig. 1 (dashed line for 1064 nm), and can be explained quantitatively by Fresnel equations for the fields.[9] Equation (2) shows that the oscillations measured in the SH signal as a function of film thickness are linearly related to $E_L'(\omega)$ so the oscillations in the data are a direct replica of the dynamic longitudinal oscillations.

The wave vectors corresponding to the oscillations seen in the data were determined by subtracting out a smooth background like that shown in Fig. 1(a) for the 1064-nm data to produce the damped oscillatory curve shown in Fig. 1(b). This curve was Fourier transformed to determine the dominant wave-vector components.[9] The experimental data points are plotted in Fig. 3, where the uncertainty represents the width of the peak in the Fourier transform. There is good agreement with the $q_s$ (surface) branch at these two wavelengths. The attenuation of the oscillations can also be measured and compared to theoretical predictions.[11] Theory predicts a

power-law falloff, with the intensity decreasing like $d^{-2}$ for large $d$ ($d$ is the film thickness). The data in Fig. 1 are best fitted with an exponent of about $-1.5$, which at this stage of our understanding should be considered as agreement. Moreover, the amplitude of the measured oscillations relative to the smooth background is seen to be larger at 1064 nm than at 532 nm. This is to be expected since the density oscillations shown in Fig. 2 are associated only with the surface contribution to the longitudinal electric field. As the frequency increases, the nonoscillatory bulklike contribution to the longitudinal field becomes stronger and therefore the relative importance of the oscillations diminishes.

In principle, oscillations corresponding to the line $q_+(\omega)$ (near $2k_F$) in Fig. 3 should also be observable. However, since these wavelengths are very close to the lattice spacing of Rb, the crystal potential could suppress these oscillations. Moreover, they will be most sensitive to surface roughness on the atomic scale.

In the above model, the oscillations are caused by a three-wave mixing process where $E_L^l(\omega)$ and $E_T^l(\omega)$ mix at the back interface to produce a signal at $2\omega$. In practice, $E_L^l(\omega)$ is likely to be modified by the linear longitudinal electric field generated at the Rb-Ag interface resulting in a standing-wave phenomenon. This wave would consist of the same oscillations as discussed above. However, it is also conceivable that the nonlinear longitudinal electric fields generated at the two interfaces interfere. The observed oscillations do not preclude this possibility since the nonlinear response to a perturbation at frequency $\omega$ leads to oscillations corresponding to both $\omega$ and $2\omega$. In the case of the 532-nm radiation, $2\omega > \omega_p$; i.e., bulk plasmon excitation in the Rb film becomes feasible.

There remain essentially two important aspects of the data which so far are not understood: The first concerns the rapid initial rise of the SH signal for coverages up to 1 monolayer. While intra-atomic resonances are likely to contribute to this enhancement[6] at very low coverages, in the monolayer regime the metallic character of the Rb film must be taken into consideration. The second aspect concerns the magnitude of the observed oscillations relative to the background SH signal. This would require a more detailed treatment of the coupling between the radiation and the longitudinal local field in the Rb film than presented here.

This work was supported by National Science Foundation Grant No. DMR-8610491, while the laser central facility was supported by National Science Foundation Materials Research Laboratory Grant No. DMR-8519059. We would like to thank L. Urbach and P. Sprunger for their help. One of us (E.W.P.) would like to thank the Guggenheim Foundation for their support.

---

[a]Permanent address: Institut für Festkörperforschung, Kernforschungsanlage, 517 Jülich, Federal Republic of Germany.

[1]P. J. Feibelman, Prog. Surf. Sci. **12**, 287 (1982).

[2]H. Levinson, E. W. Plummer, and P. J. Feibelman, Phys. Rev. Lett. **43**, 952 (1979).

[3]L. Walldén, Phys. Rev. Lett. **54**, 943 (1985).

[4]Y. R. Shen, J. Vac. Sci. Technol. B **3**, 1464 (1985).

[5]H. W. K. Tom, C. M. Mate, X. D. Zhu, J. E. Crowell, T. F. Heinz, G. Somorjai, and Y. R. Shen, Phys. Rev. Lett. **52**, 348 (1984).

[6]H. W. K. Tom, C. M. Mate, X. D. Zhu, J. E. Crowell, Y. R. Shen, and G. Somorjai, Surf. Sci. **172**, 466 (1986).

[7]T. F. Heinz, M. M. T. Loy, and W. A. Thompson, Phys. Rev. Lett. **54**, 63 (1985).

[8]D. Heskett, K.-J. Song, A. Burns, E. W. Plummer, and H.-L. Dai, J. Chem. Phys. **85**, 7490 (1986).

[9]J. Song, Ph.D thesis, University of Pennsylvania, 1988 (unpublished); a preliminary account of the data was reported in *Physical and Chemical Properties of Thin Metal Overlayers and Alloy Surfaces,* edited by D. M. Zehner and G. W. Goodman, MRS Symposium Proceedings Vol. 83 (Materials Research Society, Pittsburgh, PA, 1987).

[10]A. Zangwill and P. Soven. Phys. Rev. A **21**, 1561 (1980).

[11]A. Liebsch, Phys. Rev. B **36**, 7378 (1987).

[12]P. J. Feibelman, Phys. Rev. B **12**, 1319 (1975).

[13]See also K. Kempa, A. Liebsch, and W. L. Schaich, to be published.

[14]M. Weber and A. Liebsch, Phys. Rev. B **35**, 7411 (1987); A. Liebsch, to be published.